Pure Appl. Chem., Vol. 81, No. 9, pp. 1695–1705, 2009.
doi:10.1351/PAC-CON-08-08-31

The role of pyrimidine nucleobase excimers in DNA photophysics and photoreactivity*

Israel González-Ramírez, Teresa Climent, Juan José Serrano-Pérez, Remedios González-Luque, Manuela Merchán, and Luis Serrano-Andrés‡

Instituto de Ciencia Molecular, Universitat de València, Apartado de Correos 22085, ES-46071 Valencia, Spain

Abstract: Quantum chemical studies using the accurate CASPT2//CASSCF procedure show that π-stacked interactions in biochromophores such as pyrimidine (Pyr) DNA/RNA nucleobases pairs yield excimer-like situations which behave as precursors of processes like charge transfer (CT) or photoreactivity and are the source of the emissive properties in DNA. Examples are the CT between adjacent DNA nucleobases in a strand of oligonucleotides and the photodimerization taking place in cytosine (C) pairs leading to cyclobutanecytosine (CBC) mutants. These processes take place through nonadiabatic photochemical mechanisms whose evolution is determined by the presence and accessibility of conical intersections (CIs) and other surface crossings between different electronic states.

Keywords: bioexcimers; charge transfer; DNA lesions; DNA photochemistry; quantum chemistry.

INTRODUCTION

It is by now clearly established that π-stacked interactions between piled DNA and RNA nucleobases play a basic role in the stability, dynamics, and reactivity of the genetic material [1]. We have recently reported [2] that such types of conformations are favorable sources for the formation of excimers or exciplexes, that is, molecules which are homo- or heterodimers, respectively, associated in an excited electronic state and dissociative in the ground state [3]. The existence of excimers/exciplexes (excimer will be used as a general term hereafter) is common in different fields, including biochemistry and photobiology [1,3–5]. In particular, we have recently studied the binding energies in different states of the neutral and ionic cytosine (C) homodimer, and the existence of a bound excited state was proved by means of quantum chemical calculations in various relative conformations of the homodimer [6]. Binding and interaction change dramatically with the relative orientation of the two stacked C molecules. For instance, at the B-DNA-like type of orientations the binding energy for the low-lying excited singlet state, S_1, is just 0.11 eV, a value that increases to 0.58 eV in the so-called ^{1}(LE) conformation, a sandwich-like structure obtained by symmetrically approaching the molecules along the intermonomer distance, *R*, and to 1.10 eV in the conformation we coined $(C^*C)_{exc}$, the most stable structure for the excimer obtained by geometry optimization [6]. The stabilization is favored in the two latter orientations because of the maximum overlap obtained between the π-clouds in the homodimer. As

*Paper based on a presentation at the XXII[nd] IUPAC Symposium on Photochemistry, 28 July–1 August 2008, Gothenburg, Sweden. Other presentations are published in this issue, pp. 1615–1705.

‡Corresponding author: E-mail: Luis.Serrano@uv.es

will be shown below, the presence of so low-lying conformation in the excited state will have important consequences in the photoinduced reactivity of the nucleobases.

Before going deeper into the consequences of the excimer formation in DNA environments, and how they behave as precursors in the formation of DNA-base photoproducts [6,7], participating in the charge-transfer (CT) processes in DNA, we shall firstly establish their existence as an intrinsic property of all nucleobases, something that will be illustrated here for the homodimers of C, uracil (U), and thymine (T). Later, the importance of excimers in the rationalization of DNA emission properties and dynamics, in the formation of cyclobutane pyrimidine (Pyr) dimers, often leading to mutations, and in the CT process taking place along the DNA strands shall be discussed.

METHODOLOGY

Our methodology involves the multiconfigurational CASSCF and CASPT2 quantum chemical methods and highly accurate ANO-S-type one-electron basis sets contracted to C,N,O [3s2p1d]/H [2s1p], a strategy which has proved its accuracy [8–11]. An active space of 12 electrons in 12 orbitals was employed in the description of the CASPT2 potential energy curves (PECs) for the ground and low-lying singlet excited states of the different homodimers along the intermolecular distance between the two π-stacked systems using a C_s ground-state geometrical arrangement and C_1 symmetry to obtain the wavefunction. The inclusion of the basis set superposition error (BSSE) correction, estimated by the counterpoise correction [2], was required to get the proper description of the system. Geometry optimizations, minimum energy paths (MEPs), and determination of hypersurface crossings in the dimers were carried out initially at the CASSCF level using 16 electrons distributed among 14 molecular orbitals (MOs), that is, all the π-system except for the all-in-phase deep π-orbital localized on each monomer, which was treated as inactive. No symmetry constraints were imposed on the wavefunction. Additional computational details can be found elsewhere [2,6,7,12]. All calculations employed the MOLCAS 6.0 program quantum chemistry package [13,14].

RESULTS AND DISCUSSION

Excimer formation in π-stacked Pyr nucleobases

Our initial goal is to prove that all three Pyr nucleobases—C, T, and U—yield excimers when stacked through their π-structure. Figures 1 and 2 display the CASPT2 PECs for the ground and low-lying and triplet singlet excited states of the U homodimer along the intermolecular distance between the two π-stacked systems. A face-to-face sandwich-type arrangement has been selected because, taking into account the maximum overlap between the π-clouds, it represents the most favorable conformation to yield an excimer, which, on the other hand, is also present in other structures, for instance, the B-DNA form. As noted in Fig. 1, the lack of BSSE causes an overestimation of the states binding energies, a situation that is corrected in Fig. 2. Whereas the ground state is dissociative, the lowest singlet excited state becomes clearly bound (0.48 eV) at the corrected BSSE-CASPT2(12,12) level, with a S_1 minimum placed at $R(C_5–C_{5'}) = 2.910$ Å. In the PECs, we have chosen to monitor the intermolecular distance $R(C_5–C_{5'})$, which is particularly relevant in the formation of cyclobutane photodimers. In the figures, energies are referred to two ground-state separated U molecules. In the asymptotic limit, S_1 and S_2 become degenerate. They are related to the equivalent situations U + U* and U* + U, where U and U* represent the ground-state U and its lowest singlet excited state, respectively.

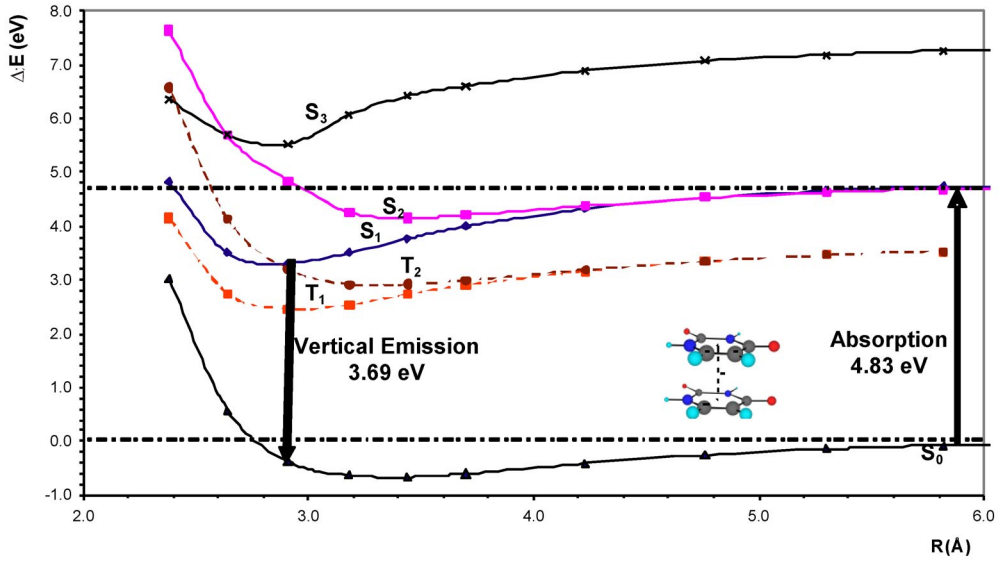

Fig. 1 CASPT2(12,12)/ANO-S C,N,O[3s2p1d]/H[2s1p] PECs built with respect to the intermolecular distance considering the center of mass of two face-to-face π-stacked U molecules.

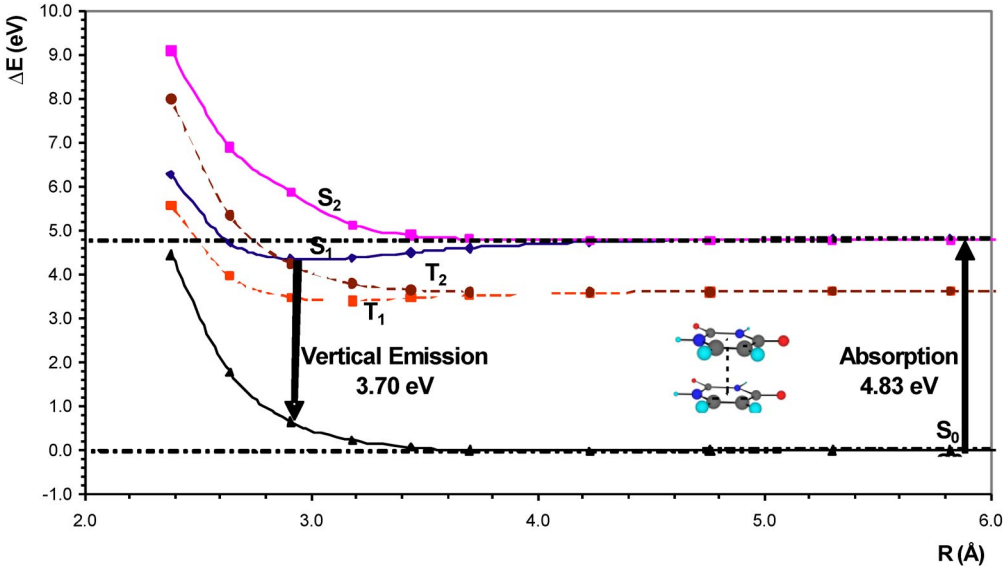

Fig. 2 Corrected BSSE-CASPT2(12,12)/ANO-S C,N,O[3s2p1d]/H[2s1p] PECs built with respect to the intermolecular distance considering the center of mass of two face-to-face π-stacked U molecules.

Similar behavior has been found for all three Pyr nucleobases. The binding energies (BSSE corrected) are compiled in Table 1.

The homodimers of the three natural Pyr nucleobases display similar behavior with respect to their binding properties, although the formation of excimers in T is hampered by the steric problems consequence of the presence of the methyl group. In particular (see Table 1) for the comparable profile as C and U, the binding energy for the T homodimer lowers to 0.36 eV and the corresponding mini-

mum takes place at a larger distance, 3.703 Å. In any case, the important conclusion obtained is that all three homodimers give rise to excimers, and, as mentioned above, the interaction occurs at many other relative orientations of the two nucleobases. Considering, therefore, the inherent flexibility of the DNA strand, there will be a large number of relative orientations in which the formation of excimers will be highly favored, even increasing the binding energy, as it was found for C (1.10 eV) upon optimization of the geometry for the S_1 state of the dimer [6].

Table 1 BSSE-corrected and -uncorrected binding energies (E_b), intermonomer distance (R_{min}), and VE for the face-to-face π-stacked homodimers of C, T, and U.

Homodimer	E_b/eV	BSSE-E_b/eV	R_{min}/Å	VE/eV
Cytosine	1.55	0.58	3.076	3.40
Thymine	1.05	0.36	3.703	4.38
Uracil	1.51	0.48	2.910	3.70

Red-shifted emission in DNA: Excimer radiative deactivation

Eisinger et al. [15] determined that in chains of oligonucleotides a source of emission was found at energies red-shifted from the weak features of the monomers, which were reported around 4.0 eV in water [16]. More detailed studies followed. For instance, the fluorescence maximum observed in aqueous solution for the dimer $d(C)_2$ and the 15-mer $d(C)_{15}$ (λ_{max} = 385 nm; 3.22 eV) [17] is considerably red-shifted as compared to that of the monomer (λ_{max} = 313 nm; 3.96 eV) [18]. Nowadays, the available experimental data for the fluorescence band maxima in dinucleotides, polynucleotides, and DNA range 3.2–3.4 eV [17].

It is, therefore, clear that π-stacked nucleobases give rise to a new source of fluorescence related to the association of the monomers. Our description of excimers in the homodimers of the Pyr nucleobases at different orientations of the moieties and the CASPT2 computed vertical emissions (VEs) supports the excimer origin of the red-shifted fluorescence observed in Pyr oligonucleotides [15,17], whereas preliminary studies indicate that excimers are also present for purine nucleobase dimers. Our best estimates have differences near 0.2 eV with respect to the recorded emission maxima, however, it is worth recalling that the computed vertical transition does not have experimental counterpart, and for a truly correct comparison with experiment, vibrational resolution of the band should be computed in order to determine the band maximum.

The evidence of the excimer origin of the emissive properties of DNA highlights the importance of π-stacking and excimer formation in the modulation of DNA relaxation dynamics, which will combine emission with nonradiative decays through accessible CIs connecting the ground and low-lying singlet excited state—such as those found for the monomers at 3.6 (C), 3.9 (T), 4.0 (U), 4.0 (adenine, A), and 4.3 eV (guanine, G) [7,11,19–21]—favoring hole and electron transfer along the strand, and formation of lesions as covalently bound Pyr dimers [1,6].

Charge transport along the DNA strand: Micro-hopping mechanism

Nucleobase cations and anions can be formed via direct ionization of the DNA strand as primary radical product, by means of the exposure of living matter to ionizing radiation and, also indirectly, as secondary radical products of the nucleobase interaction with reactive species present in DNA and its vicinity, that is, endogenous compounds that have been originated from irradiation of other DNA components or water: sugar and phosphate radicals, $^{\bullet}OH$, the hydrated electron, $H^{\bullet}$, and H_3O^+ [22,23]. The energy required for the formation of charged nucleobases, related to the corresponding ionization potential (IP) and electron affinity (EA), has been evaluated both experimentally and theoretically. Once

the charged DNA bases are formed, the produced hole or electron can migrate up to long distances through the π-stacked structure of the double helix [24,25]. This phenomenon is known in general as charge transport or transfer (CT), and it is usually denoted hole transfer (HT) and excess electron transfer (EET) when it takes place under oxidative and reductive stress, respectively. Because of its biological implications and its technological and medical applications, CT in DNA has been during the last decades an area of increasing interest [26–29].

Whereas it is currently established by using different spectroscopic, biochemical, electrochemical, and photophysical studies that DNA provides a favorable medium for CT [30–33], the detailed mechanism on how it takes place is not yet known. The available models have been particularly focused on HT and, among the different hypotheses suggested, three main mechanisms have been put forward: (1) coherent single-step tunneling process between the initial and final charged nucleobases [34–36] (2) random-walk multistep hopping process between the initial and final sites mediated by G [37–39] and, in special cases, by A [40], (3) and polaron-like hopping process [41–44]. We have recently applied the highest available levels of theory to produce accurate theoretical (in vacuo) values for IPs and EAs [45,46], and our goal here is to summarize our preliminary efforts to establish a comprehensive model to rationalize at molecular level the CT process. Focusing on the HT type of mechanism, and in order to get further insight into the mechanism of CT, we have analyzed at the CASPT2 level the lowest doublet states of different oxidized nucleobase homo- and heterodimers in different orientations, from the highly overlapped π-stacked face-to-face arrangement (see Figs. 1 and 2) to the B-DNA form (see Figs. 3 and 4) and their evolution upon different displacements [47–49]. As an illustration we show here the case of the cationic A–C heterodimer ($C_{3'}A_{5'}^+$) in the B-DNA form [12] along the rise coordinate, that is, the displacement along the DNA helix axis [48].

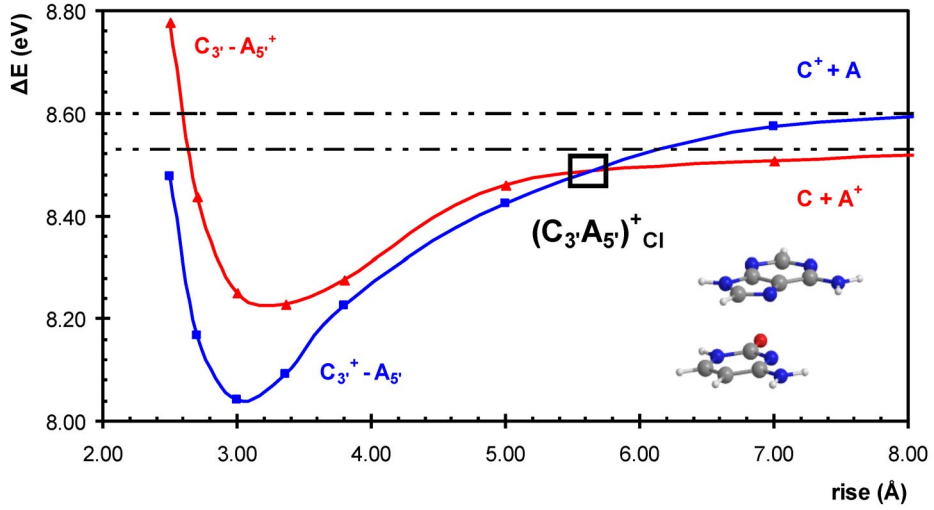

Fig. 3 BSSE-corrected CASPT2/ANO-S C,N,O [321]/H [21] PECs, built with respect to the intermonomer distance (rise) for the two low-lying doublet states of the oxidized C–A heterodimer $(C_{3'}A_{5'})^+$. The CI between the ground and lowest excited state of the dimer is represented by $(C_{3'}A_{5'})^+_{CI}$ and marked with a black square.

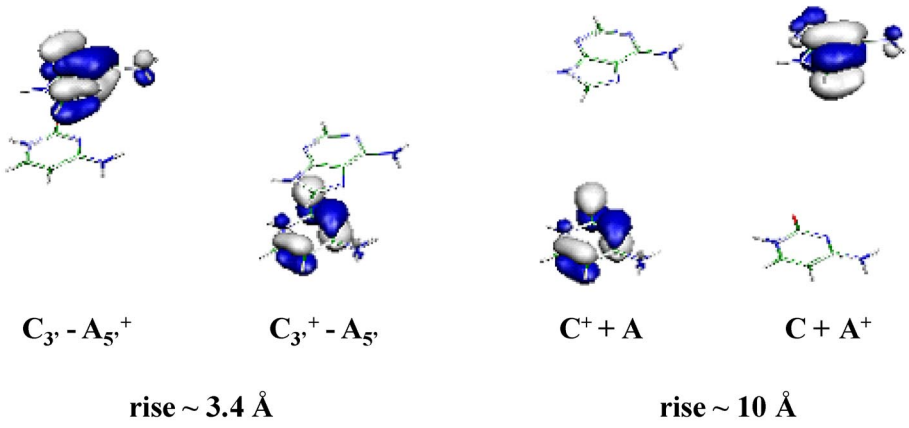

Fig. 4 Singly occupied natural orbitals (SONOs) of the ground and lowest excited state of the cationic B-DNA form of the A–C heterodimer $(C_{3'}A_{5'})^{+}$ at a geometry close to the average distance in DNA (3.4 Å) (left) and at large distances (right).

By inspection of the PECs for the $C_{3'}A_{5'}^{+}$ heterodimer, it is evident that an oxidized C is strongly stabilized by the presence of A. As it can be seen in Fig. 3, in the heterodimer analyzed here, $(C_{3'}A_{5'}^{+})$, the cationic C and A are bound by the adjacent neutral nucleobase with decreases in their IPs of 0.56 eV at *rise* = 3.00 Å and 0.30 eV at *rise* = 3.36 Å, respectively. Since the Pyr nucleobase is more stabilized than the purine one and such stabilization is higher than the difference between the IPs of the isolated nucleic bases, the two low-lying states of the system, $C_{3'}^{+}A_{5'}$ and $C_{3'}A_{5'}^{+}$, which are characterized by the location of the hole in the C or A, respectively, cross-over in a point that takes place at intermolecular distances around 5.5–6.0 Å and corresponds to the conical intersection (CI) that mediates the HT between both nucleobases, $(C_{3'}A_{5'})^{+}_{CI}$. This result implies that the order of the IPs of C and A is inverted when these nucleic bases appear in adjacent positions of a DNA chain, and therefore the electron is removed from the Pyr nucleobase when the A–C heterodimer is oxidized. The remaining hole of the oxidation can be filled again by the promotion of one electron from the A partner by means of a thermally activated increase of the intermolecular distance between both nucleobases through the $(C_{3'}A_{5'})^{+}_{CI}$. This behavior is illustrated by the composition of the singly occupied MOs displayed in Fig. 4. Similar conclusions can be obtained by studying other nucleobase dimers upon other displacements, isolated or within the oligomer strand and under different environmental conditions, something which is currently under analysis by using QM/MM procedures. In all cases, the cornerstone of the mechanism is the presence of PEC CI crossings enabling ultrafast hole (or electron) transfer to take place. It is also true that the degree of transfer between the two states will be modulated by the strength of the electronic coupling between them, which is, together with the energy degeneration, the main condition for efficient charge or energy transfer. Comparison between the strength of the energy coupling between the different nucleobase dimers will be the goal of future research.

As a conclusion, the formation of stable excimer-like structures, revealed to be an intrinsic property of stacked nucleobases, also provides the framework to assemble the process of charge migration within the same basic unique scheme or unified theory. In this context, we propose a *micro-hopping* mechanism for CT along a single strand of nucleobase molecules formulated as a sequence of steps. Starting from an arrangement of π-stacked monomers at typical intermolecular distances of 3.1–3.4 Å, and considering the inherent flexibility of the DNA helix, in each step the two adjacent nucleobases may change their relative orientations by, for instance, increasing and decreasing their rise or twisting distance, by means of a thermally activated process, leading the system to reach accessible CIs between the lowest doublet states of the system and to transfer the excess electron (or hole charge) between the two molecules in an ultrafast manner. Therefore, charge migrates from an initial charged nucleobase to

the adjacent moiety in one step and between the initial and final charged DNA-sites in a sequence of such steps, thus making possible the CT process along the strand. That the process is more or less favorable will be surely related to the intrinsic properties of the nucleotide. It is therefore understandable that G sites, displaying the highest IPs, behave as hole charge trapping locations where the CT process is hindered, because they need a strongly distorted interacting conformation in order to cross with another state and transfer the hole to the neighbor moiety. Further research has to be performed in order to fully validate this hypothesis, extending the study to all combination of nucleobases and environments and considering the role of the Watson–Crick nucleobase pairs.

Photoreactivity in DNA: Formation of mutated Pyr dimers

One of the main motivations for studying the excited states of nucleic acids relies on the observation that UV illumination causes lesions and mutations due to photochemical modifications, the most common involving cycloaddition reactions of Pyrs T and C. Although the production of T–T cyclobutane dimers is most frequent, those involving C lead to mutation. T dimerization has recently been determined [50] to be an ultrafast reaction along the singlet manifold, whereas time-resolved studies of T dimer formation [51] show that direct excitation of $(dT)_{20}$ leads to cyclobutane T dimers (T <> T) in less that 200 ns with a remarkably absence of any triplet absorption from the transient spectra of the oligonucleotide. These evidences are in contrast to previous suggestions about the role of triplet states in DNA chemistry, in particular on the formation of Pyr complexes, Pyr <> Pyr [52], and are also at odds with the well-known dimerization at the bipyrimidine sites under triplet photosensitization conditions [53]. Effective population of the triplet manifold is feasible, and it has been documented in detail for C [54], U [55], and T [56] along the ultrafast internal conversion channel. It is therefore not surprising that in addition to the presence of singlet excimer states which will behave as precursors of the photodimerization process, we have found corresponding triplet excimer states. For instance, in the C homodimer, the binding energy for the lowest triplet state computed at the CASPT2 level (plus BSSE) is 0.22 eV, with a predicted VE (phosphorescence) of 3.23 eV and a 0–0 triplet–singlet transition of 3.44 eV. Consequently, it is concluded that the triplet excimer is also bound, although the binding energy is reduced about 60 % with respect to singlet excimer. The possibility of excimer formation arises from the Watson–Crick structure in which hydrogen-bonded pairs A–T and G–C are situated inside a double helix, the backbone formed by two sugar-phosphate chains. One turn of the helix involves 10 base pairs and is 34 Å high. Thus, the interplanar distance between neighboring base pairs is about 3.4 Å, a value that is often found in excimer-type organic crystals [3].

Because of the increased stability of the lowest excited state, geometries around the face-to-face sandwich-type structure can be considered as the best candidates as precursors of photodimers. It seems that the ideal twist angle between successive base pairs makes the geometry of the B-DNA (and A-DNA) nonreactive. According to recent experimental evidence, the static Pyr-Pyr conformations and not conformational motions after photoexcitation determines the formation of (Pyr <> Pyr) photoproducts. Within the model proposed by Schreier et al. [50], the relatively smaller degree of flexibility of A-DNA compared to B-DNA to achieve the right orientations that become prone to react has been related to the greater resistance of A-DNA to (Pyr <> Pyr) formation. As shown by these authors, dimerization occurs only for T residues that are already in a reactive arrangement at the instant of excitation because the rate of formation by favorably oriented T pairs is much faster that the rate of orientation change. A similar situation can therefore be assumed in C oligomers. We have taken the face-to-face arrangements, both for the singlet and triplet excimers, as the starting point for the study of the dimerization reaction occurring along the singlet and triplet manifold, respectively, in order to clarify at the molecular level the controversial and poorly understood mechanism of photodimer formation.

Figure 5 displays a scheme, based on the CASPT2 results, on the photodimerization of two C molecules taking place along both the singlet and the triplet manifold. The photoreactions taking place belong to the class of the [2+2] photocycloadditions. Starting from the triplet, MEP computations from

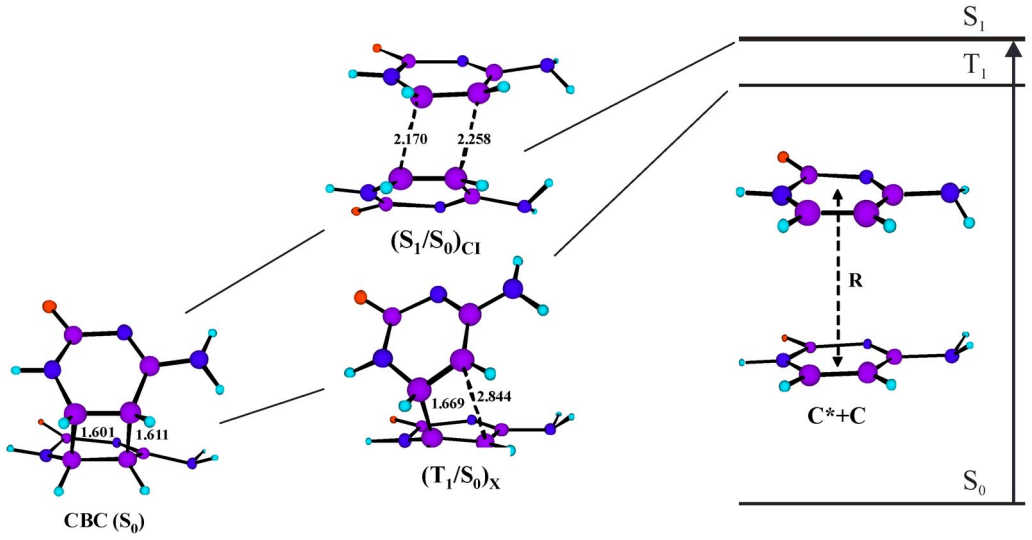

Fig. 5 Scheme based on CASPT2 calculations for the photoinduced formation of a CBC from a π-stacked C excimer (C* + C) and along the singlet and triplet manifold, involving a CI $(S_1/S_0)_{CI}$ and a singlet–triplet intermediate $(T_1/S_0)_X$, respectively.

the face-to-face arrangement lowest-energy minima of T_1 lead directly in a barrierless fashion to a triplet step-wise intermediate, which is characterized by the formation of a single covalent intermonomer bond computed to be 1.669 Å, whereas the other intermonomer CC distance remains elongated, about 2.8 Å. Remarkably, at this optimal structure the ground state of the system becomes degenerate. In other words, the triplet state is coincident with a triplet–singlet crossing, $(T_1/S_0)_X$, a region of the hypersurface where decay to the ground state becomes particularly favored. Such singlet–triplet degeneracy can be understood on the basis of the biradical character of the triplet–singlet states, having the unpaired electrons located on the bound C atoms. The intermediate triplet state lies 2.70 eV above two ground-state C molecules, an energy difference that can be considered a lower bound for the triplet energy of C in DNA.

It can be envisaged that exogenous photosensitizers could populate the relaxed triplet state of the monomer, which will subsequently evolve toward the intermediate and then toward the formation of the mutated dimers. Thus, the required energy can be related to the threshold observed experimentally for a given compound to become a potential DNA photodamager via (C <> C) or (T <> T) formation. The computed result for the singlet–triplet crossing structure of C, 2.70 eV, is fully consistent with the triplet energy of T in DNA deduced experimentally, 2.80 eV [53]. The intermediate represents, thus, a channel for photodimer formation from the triplet state of π-stacked C (and presumably also for T) in DNA and provides the basic understanding of potential photogenotoxicity via triplet–triplet sensitization. The efficiency of the overall process along the triplet manifold will be affected by the magnitude of the spin-orbit coupling (SOC), which is directly related to the efficiency of the intersystem crossing (ISC) process, and that would strongly rely on the actual environment of the biopolymer.

Regarding the mechanism of C photodimer formation along the singlet manifold, and in line with the similar excited-state [2+2] cycloadditon reactions of two ethene molecules [57], a CI is the funnel of decay toward ground-state cyclobutane C dimer (CBC) from the singlet excimer. Computations from different unrelaxed excimer lead to such CI structure. The process in the triplet manifold is also expected to follow a steepest descent path as it occurs along the singlet hypersurface. Thus, the current view supports the hypothesis that the dimerization photoreaction of two C molecules occurs barrierless, both on the singlet and triplet hypersurfaces. It would depend on the experimental conditions whether

the singlet or triplet mechanism becomes activated, fully operative, or even competitive with each other. The different mechanisms proposed in the literature involve singlet and triplet states of the monomers and vertical stacking to account for dimerization in solution and solid state, respectively. All those are here supported on the basis of CASPT2 results [6,58,59]. The efficiency of the photodimerization would markedly depend on the experimental conditions (solvent, aggregation conditions, pH, degree of hydratation), the sequence of nucleotides, the type (A-, B- C-like) of DNA conformation [50,52]. Also important for the relative efficiency of the dimer formation is the presence of relaxed excimer structures at energies lower than the CI, as it occurs in C in contrast to T, a feature that lowers the formation yield of CBC. In fact, if dimer formation occurs with reasonable yields between monomeric solute molecules in solution, the dimer must have a triplet precursor, because singlet lifetimes simply are not long enough to permit excited bimolecular reactions to occur [60]. Nevertheless, as Eisinger and Shulman have emphasized [60], the same reaction which proceeds via triplet state in solution may have a singlet-state precursor when the biochromophores are held together, as is the case in frozen solutions or in a biopolymer. Theory predicts that the photoinduced reactions both on the singlet and triplet hypersurfaces are essentially barrierless, and singlet and triplet excimers play an active role in the photophysics outcome and in the photochemical properties of C-containing biopolymers. The present results also offer a nice rationale to the known fact that Pyr dimers are formed under triplet photosensitization conditions [52].

ACKNOWLEDGMENTS

Financial support is acknowledged from projects CTQ2007-61260 and CSD2007-0010 Consolider-Ingenio in Molecular Nanoscience of the Spanish MEC/FEDER. I.G.R. acknowledges a Ph.D. grant from the Spanish MEC (FPI).

REFERENCES

1. C. E. Crespo-Hernández, B. Cohen, P. M. Hare, B. Kohler. *Chem. Rev.* **104**, 1977 (2004).
2. G. Olaso-González, D. Roca-Sanjuán, L. Serrano-Andrés, M. Merchán. *J. Chem. Phys.* **125**, 231102 (2006).
3. J. B. Birks. *Rep. Prog. Phys.* **38**, 903 (1975).
4. W. Klöpffer. "Intramolecular excimers", in *Organic Molecular Photophysics*, J. B. Birks (Ed.), p. 357, Wiley-Interscience, London (1973).
5. G. Olaso-González, M. Merchán, L. Serrano-Andrés. *J. Phys. Chem. B* **110**, 24734 (2006).
6. D. Roca-Sanjuán, G. Olaso-González, I. González-Ramírez, L. Serrano-Andrés, M. Merchán. *J. Am. Chem. Soc*. **130**, 10768 (2008).
7. L. Serrano-Andrés, M. Merchán. "Photostability and photoreactivity in biomolecules: Quantum chemistry of nucleic acid base monomers and dimers", in *Radiation Induced Molecular Phenomena*, J. Leszczynski, M. Shukla (Eds.), Springer, Berlin (2008).
8. K. Andersson, P.-Å. Malmqvist, B. O. Roos. *J. Chem. Phys.* **96**, 1218 (1992).
9. L. Serrano-Andrés, M. Merchán, I. Nebot-Gil, R. Lindh, B. O. Roos. *J. Chem. Phys*. **98**, 3151 (1993).
10. B. O. Roos, K. Andersson, M. P. Fülscher, P.-Å. Malmqvist, L. Serrano-Andrés, K. Pierloot, M. Merchán. *Adv. Chem. Phys.* **93**, 219 (1996).
11. L. Serrano-Andrés, M. Merchán, A. C. Borin. *Proc. Natl. Acad. Sci. USA* **103**, 8691 (2006).
12. D. Roca-Sanjuán, L. Serrano-Andrés, M. Merchán. *Chem. Phys.* **349**, 188 (2008).
13. G. Karlström, R. Lindh, P.-Å. Malmqvist, B. O. Roos, U. Ryde, V. Veryazov, P.-O. Widmark, M. Cossi, B. Schimmelpfennig, P. Neogrady, L. Seijo. *Comp. Mater. Sci.* **28**, 222 (2003).
14. V. Veryazov, P.-O. Widmark, L. Serrano-Andrés, R. Lindh, B. O. Roos. *Int. J. Quantum Chem.* **100**, 626 (2004).
15. J. Eisinger, M. Guéron, R. G. Shulman, T. Yamane. *Proc. Natl. Acad. Sci. USA* **55**, 1015 (1966).

16. P. R. Callis. *Annu. Rev. Phys. Chem.* **34***,* 329 (1983).
17. R. Plessow, A. Brockhinke, W. Eimer, K. Kohse-Höinghaus. *J. Phys. Chem. B* **104**, 3695 (2000).
18. P. R. Callis. *Annu. Rev. Phys. Chem.* **34**, 329 (1983).
19. M. Merchán, R. González-Luque, T. Climent, L. Serrano-Andrés, E. Rodríguez, M. Reguero, D. Peláez. *J. Phys. Chem. B* **110**, 26471 (2006).
20. L. Serrano-Andrés, M. Merchán, A. C. Borin. *Chem.—Eur. J.* **12**, 6559 (2006).
21. L. Serrano-Andrés, M. Merchán, A. C. Borin. *J. Am. Chem. Soc.* **130**, 2473 (2008).
22. M. Aida, M. Kaneko, M. Dupuis. In *Computational Molecular Biology*, J. Leszczynski (Ed.), Elsevier, Amsterdam (1999).
23. S. D. Wetmore, L. A. Eriksson, R. J. Boyd. In *Theoretical Biochemistry: Processes and Properties of Biological Systems*, L. A. Eriksson (Ed.), Elsevier, Amsterdam (2001).
24. M. E. Núñez, D. B. Hall, J. K. Barton. *Chem. Biol*. **6**, 85 (1999).
25. D. Ly, L. Sanii, G. B. Schuster. *J. Am. Chem. Soc*. **121**, 9400 (1999).
26. S. Delaney, J. K. Barton. *J. Org. Chem*. **68**, 6475 (2003).
27. E. M. Boon, J. K. Barton. *Curr. Opin. Struct. Biol*. **12**, 320 (2002).
28. C. R. Treadway, M. G. Hill, J. K. Barton. *Chem. Phys*. **281**, 409 (2002).
29. E. B. Starikov. *Int. J. Quant. Chem*. **77**, 859 (2000).
30. M. E. Núñez, J. K. Barton. *Curr. Opin. Chem. Biol*. **4**, 199 (2000).
31. G. B. Schuster. *Acc. Chem. Res*. **33**, 253 (2000).
32. B. Giese. *Annu. Rev. Biochem*. **71**, 51 (2002).
33. F. D. Lewis, R. L. Letsinger, M. R. Wasielewski. *Acc. Chem. Res*. **34**, 159 (2001).
34. R. A. Marcus, N. Sutin. *Biochim. Biophys. Acta* **811**, 265 (1985).
35. M. Ratner. *Nature* **397**, 480 (1999).
36. J. Jortner, M. Bixon, T. Langenbacher, M. E. Michel-Beyerle. *Proc. Natl. Acad. Sci. USA* **95**, 12759 (1998).
37. B. Giese. *Acc. Chem. Res*. **33**, 631 (2000).
38. Y. A. Berlin, A. L. Burin, M. A. Ratner. *J. Am. Chem. Soc*. **123**, 260 (2001).
39. J. Joseph, G. B. Schuster. *J. Am. Chem. Soc*. **128**, 6070 (2006).
40. B. Giese, J. Amaudrut, A.-K. Köhler, M. Spormann, S. Wessely. *Nature* **412**, 318 (2001).
41. P. T. Henderson, D. Jones, G. Hampikian, Y. Kan, G. B. Schuster. *Proc. Natl. Acad. Sci. USA* **96**, 8353 (1999).
42. E. M. Conwell, S. V. Rakhmanova. *Proc. Natl. Acad. Sci. USA* **97**, 4556 (2000).
43. E. M. Conwell, S. M. Bloch. *J. Phys. Chem. B* **110**, 5801 (2006).
44. E. M. Conwell, S. M. Bloch, P. M. McLaughlin, D. M. Basko. *J. Am. Chem. Soc*. **129**, 9175 (2007).
45. D. Roca-Sanjuán, M. Rubio, M. Merchán, L. Serrano-Andrés. *J. Chem. Phys.* **125**, 084302 (2006).
46. D. Roca-Sanjuán, M. Merchán, L. Serrano-Andrés, M. Rubio. *J. Chem. Phys*. **129**, 095104 (2008).
47. R. Chandrasekaran, S. Arnott. In *Landolt-Börnstein Numerical Data and Functional Relationships in Science and Technology, Group VII/1b, Nucleic Acids*, W. Saenger (Ed.), p. 31, Springer-Verlag, Berlin (1989).
48. S. Arnott. In *Oxford Handbook of Nucleic Acid Structure*, S. Neidle (Ed.), p. 1, Oxford University Press, Oxford (1999).
49. X.-J. Lu, W. K. Olson. *Nucleic Acids Res.* **31**, 5108 (2003).
50. W. J. Schreier, T. E. Schrader, F. O. Koller, P. Gilch, C. E. Crespo-Hernández, V. N. Swaminathan, T. Carell, W. Zinth, B. Kohler. *Science* **315**, 625 (2007).
51. S. Marguet, D. Markovitsi. *J. Am. Chem. Soc.* **127**, 5780 (2005).
52. J. Cadet, P. Vigny. "The photochemistry of nucleic acids", in *Bioorganic Photochemistry*, H. Morrison (Ed.), John Wiley, New York (1990).

53. F. Bosca, V. Lhiaubet-Vallet, M. C. Cuquerella, J. V. Castell, M. A. Miranda. *J. Am. Chem. Soc.* **128**, 6318 (2006).
54. M. Merchán, L. Serrano-Andrés, M. A. Robb, L. Blancafort. *J. Am. Chem. Soc.* **127**, 1820 (2005).
55. T. Climent, R. González-Luque, M. Merchán, L. Serrano-Andrés. *Chem. Phys. Lett.* **441**, 327 (2007).
56. J. J. Serrano-Pérez, R. González-Luque, M. Merchán, L. Serrano-Andrés. *J. Phys. Chem. B* **111**, 11880 (2007).
57. F. Bernardi, M. Olivucci, M. A. Robb. *Acc. Chem. Res.* **23**, 405 (1990).
58. M. Boggio-Pasqua, G. Groenhof, L. V. Schäfer, H. Grubmüller, M. A. Robb. *J. Am. Chem. Soc.* **129**, 10996 (2007).
59. L. Blancafort, A. Migani. *J. Am. Chem. Soc.* **129**, 14540 (2007).
60. J. Eisinger, R. G. Shulman. *Science* **161**, 1311 (1968).